International Journal of Mass Spectrometry 290 (2010) 145–147

Contents lists available at ScienceDirect

International Journal of Mass Spectrometry

journal homepage: www.elsevier.com/locate/ijms

Short communication

The spiral main path electric deflector as a time-of-flight mass analyzer

Damaschin Ioanoviciu*

Physics Faculty, Babes-Bolyai University, M. Kogalniceanu Str.1, 400084 Cluj-Napoca, Romania

ARTICLE INFO

Article history:
Received 17 August 2009
Received in revised form
26 November 2009
Accepted 3 December 2009
Available online 16 December 2009

Keywords:
Cylindrical condenser
Logarithmic spiral
Time-of-flight
Transfer matrix element

ABSTRACT

The logarithmic main path cylindrical condenser can be used as time-of-flight mass analyzer. To describe its flight-time properties the transfer matrix elements up to second order were derived. The such completed logarithmic main path condenser transfer matrix allows the determination of the configurations of the time-of-flight mass spectrometers ensuring energy focusing or initial velocity focusing by delayed extraction, while the ion packet is drastically compressed along its path.

1. Introduction

The transversal focusing of the ions inside an electrostatic field created by two cylindrical electrodes with logarithmic spiral cross-sections was discussed in [1] and [2] at a second order accuracy level. Such condensers can serve to compress radially broad ion beams or packets as it is useful to focus ions resulted from cosmic dust impact on large sensitive areas [3]. Below, the time-of-flight, longitudinal, matrix elements are given for a complete second order matrix description of the spiral main path condenser ion optics (completing a matrix like that given in Table 1 of [4]).

2. Method

The derivations of the flight time followed the general trend of the calculations pursued in [4]. The flight time of an arbitrary ion, t, of velocity v, through the condenser is

$$t = \frac{l}{v_0} = \int_0^{\varphi} \frac{ds}{v} = \int_0^{\varphi} (r^2 + r'^2 + z'^2)^{1/2} \frac{d\theta}{v} \tag{1}$$

The involved symbols are as follows φ angle of the deflecting sector (Fig. 1), ds ion path element, r, θ, z cylindrical coordinates, "prime" means derivation with respect to θ, index "zero" refers to the main path ion, l_0/v_0 being its flight time through the condenser.

Before to proceed to the integration, the following substitutions were made:

(a) $r = \mathrm{Re}\, xp(\mu\theta) - y$ with $y = \Sigma D_i S_i + \Sigma D_{jk} S_j S_k$ taken from [1] where S_i are the following small quantities: y distance, α angle, δ relative energy deviation (in the deflection plane), β angle off median plane, all related to the main path ion trajectory.
D_i and D_{jk} were taken from [1] except $D_{\delta\delta}$ with its corrected value given in the attached errata.

(b) r' and z' resulted by simple derivation of the expressions of r and $z = \Sigma D_i S_i$

(c) $v = v_0 \sqrt{([1 + (2/(1+\mu^2))(\mu\theta - \ln(r/R))])/(1+\gamma)}$ with $|\mu| = \sqrt{(m_0 v_0^2/e|E_0|R) - 1}$ E_0 being the radial electrostatic field at $r = R$, γ the relative mass deviation.

These substitutions performed, the expression under integral has been developed in series after the small quantities y/R, α, δ, γ, z/R and β involved, only terms small of second order being retained.

3. Time-of-flight transfer matrix elements

After integration we obtain with a second order accuracy:

$$l = l_0 + (l/i)S_i + (l/jk)S_{jk} \tag{2}$$

The following S_i, S_{jk} flight-time matrix elements resulted:

$$\left(\frac{l}{y}\right) = \frac{[2ck\mu + s(\mu^2+4)]\exp(\mu\varphi/2) - 2k\mu}{2k\sqrt{1+\mu^2}} \tag{3}$$

$$\left(\frac{l}{\alpha}\right) = R\sqrt{1+\mu^2}\,\frac{2k - \exp(\mu\varphi/2)(2ck - 3\mu s)}{2k} \tag{4}$$

* Tel.: +40 264 588 439; fax: +40 264 420 042.
E-mail address: dioanoviciu@gmail.com.

1387-3806/$ – see front matter © 2009 Elsevier B.V. All rights reserved.
doi:10.1016/j.ijms.2009.12.004

$$\left(\frac{l}{\delta}\right) = R\sqrt{1+\mu^2}\,\frac{2k\exp(\mu\varphi)(1+\mu^2) - \mu\exp(\mu\varphi/2)(2ck\mu + s(\mu^2+4)) - 2k}{4k\mu} \tag{5}$$

$$\left(\frac{l}{\gamma}\right) = R\sqrt{1+\mu^2}\,\frac{\exp(\mu\varphi)-1}{2\mu} \tag{6}$$

$$\left(\frac{l}{yy}\right) = \exp\left(\frac{\mu\varphi}{2}\right)(\mu^2-1)\frac{2ck\mu + s(\mu^2-12)}{4Rk(9-\mu^2)\sqrt{1+\mu^2}} + \frac{2c^2k\mu(\mu^6-9\mu^4-2\mu^2+98) + sc(\mu^2-8)(\mu^6-5\mu^4-6\mu^2-30) - k\mu(\mu^6-10\mu^4-3\mu^2+188)}{2Rk(\mu^2-9)(\mu^2-8)(1+\mu^2)^{3/2}} \tag{7}$$

$$\left(\frac{l}{y\alpha}\right) = \exp\left(\frac{\mu\varphi}{2}\right)\frac{2ck(\mu^4-3\mu^2+6) - \mu s(\mu^2-4)(\mu^2-5)}{k(9-\mu^2)(1+\mu^2)^{3/2}} + 2\frac{2c^2k(\mu^6-8\mu^4+\mu^2-30) + \mu sc(\mu^6-10\mu^4-3\mu^2+128) - k(3\varphi\mu^3(\mu^2-9) + (\mu^2+3)(\mu^4-8\mu^2-4)}{k(\mu^2-9)(\mu^2-8)(1+\mu^2)^{3/2}} \tag{8}$$

$$\left(\frac{l}{y\delta}\right) = \exp\left(\frac{\mu\varphi}{2}\right)(\mu^2-1)\sqrt{1+\mu^2}\,\frac{2ck\mu + s(\mu^2-12)}{4k(\mu^2-9)} + \frac{2c^2k\mu(\mu^6-9\mu^4-2\mu^2+98) + sc(\mu^2-8)(\mu^6-5\mu^4-6\mu^2-30) - k\mu(\mu^6-10\mu^4-3\mu^2+188)}{2k(9-\mu^2)(\mu^2-8)\sqrt{1+\mu^2}} \tag{9}$$

$$\left(\frac{l}{y\gamma}\right) = \frac{\exp(\mu\varphi/2)[2ck\mu + s(\mu^2+4)] - 2k\mu}{4k\sqrt{1+\mu^2}} \tag{10}$$

$$\left(\frac{l}{\alpha\alpha}\right) = \mathrm{Re}\,xp\left(\frac{\mu\varphi}{2}\right)\sqrt{1+\mu^2}\,\frac{10ck\mu - 3s(\mu^2-4)}{k(9-\mu^2)} + R\sqrt{1+\mu^2}\,\frac{2c^2k\mu(11\mu^2-79) + sc(\mu^2-8)(\mu^2-5)(2\mu^2-3) - 2k\mu(1+\mu^2)}{2k(\mu^2-9)(\mu^2-8)} \tag{11}$$

$$\left(\frac{l}{\alpha\delta}\right) = \mathrm{Re}\,xp\left(\frac{\mu\varphi}{2}\right)\frac{2ck(\mu^4+2\mu^2+21) + \mu s(\mu^4-6\mu^2-67)}{4k(\mu^2-9)\sqrt{1+\mu^2}} + R\frac{4c^2k(\mu^6-8\mu^4+\mu^2-30) + 2\mu sc(\mu^6-10\mu^4-3\mu^2+128) - k(6\varphi\mu^3(\mu^2-9) + 3\mu^6-26\mu^4-\mu^2+48)}{2k(9-\mu^2)(\mu^2-8)\sqrt{1+\mu^2}} \tag{12}$$

$$\left(\frac{l}{\alpha\gamma}\right) = R\sqrt{1+\mu^2}\,\frac{2k - \exp(\mu\varphi/2)(2ck - 3\mu s)}{4k} \tag{13}$$

$$\left(\frac{l}{\delta\delta}\right) = R\left\{\exp(\mu\varphi)\frac{(1+\mu^2)^{5/2}}{8\mu} + \exp\left(\frac{\mu\varphi}{2}\right)(1+\mu^2)^{3/2}\frac{2ck\mu(\mu^2-5) + s(\mu^4-9\mu^2-12)}{8k(9-\mu^2)}\right\} + R\sqrt{1+\mu^2}\,\frac{2c^2k\mu^2(\mu^6-9\mu^4-2\mu^2+98)}{8k\mu(\mu^2-9)(\mu^2-8)} + R\sqrt{1+\mu^2}\,\frac{\mu sc(\mu^2-8)(\mu^6-5\mu^4-6\mu^2-30) - k(\mu^8-9\mu^6-19\mu^4+243\mu^2+72)}{8k\mu(\mu^2-9)(\mu^2-8)} \tag{14}$$

$$\left(\frac{l}{\delta\gamma}\right) = R\sqrt{1+\mu^2}\,\frac{2k\exp(\mu\varphi)(1+\mu^2) - \mu\exp(\mu\varphi/2)[2ck\mu + s(\mu^2+4)] - 2k}{8k\mu} \tag{15}$$

$$\left(\frac{l}{\gamma\gamma}\right) = R\sqrt{1+\mu^2}\,\frac{1-\exp(\mu\varphi)}{8\mu} \tag{16}$$

$$\left(\frac{l}{\beta\beta}\right) = R\sqrt{1+\mu^2}\exp\left(\frac{\mu\varphi}{2}\right)\frac{2ck\mu + s(\mu^2+4)}{4k} - R\frac{\exp(\mu\varphi)(\mu^4+3\mu^2+1) - 2\mu^2 - 1}{2\mu\sqrt{1+\mu^2}} \tag{17}$$

with $c = \cos(k\varphi)$, $s = \sin(k\varphi)$, $k = (8-\mu^2)^{1/2}/2$ if $\mu < 2(2)^{1/2}$.

Correction for oblique ion entry and exit at the electric field effective boundary is provided by the following transfer matrix elements to be added to those for y and z in the fringing fields given in [1].

At the entry

$$\left(\frac{l}{y}\right) = \mu, \quad \left(\frac{l}{y\delta}\right) = -\frac{\mu}{2}, \quad \left(\frac{l}{\gamma}\right) = \frac{\mu}{2}, \quad \left(\frac{l}{y\alpha}\right) = \mu^2 \tag{18}$$

At the exit:

$$\left(\frac{l}{y}\right) = -\frac{\mu}{\sqrt{1+\mu^2}}, \quad \left(\frac{l}{y\delta}\right) = \frac{\mu}{2\sqrt{1+\mu^2}}, \quad \left(\frac{l}{y\gamma}\right) = -\frac{\mu}{2\sqrt{1+\mu^2}} \tag{19}$$

Not explicitly mentioned matrix elements vanish.

4. Checking expressions for the limiting case $\mu = 0$

The above matrix elements transform into those for the usual circular cylinder condenser at the limit for $\mu \to 0$. The matrix elements thus resulted were checked against those for cylindrical condensers coming from the results of Ref. [5] corroborated with those of [6] and [7].

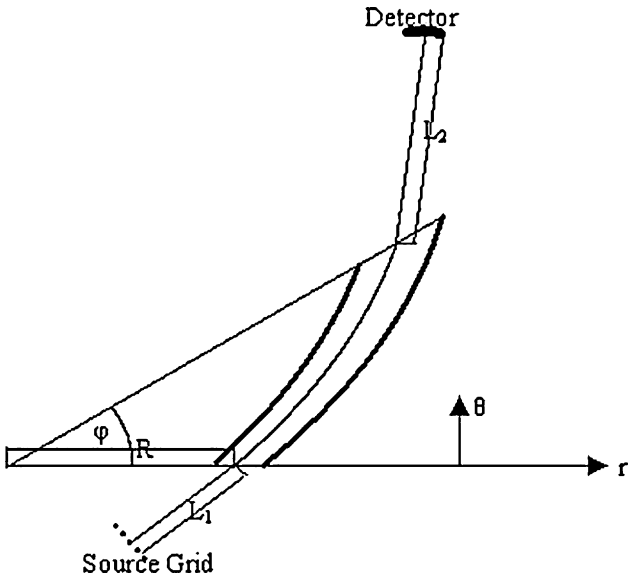

Fig. 1. Basic parameters defining the geometry of a time-of-flight mass spectrometer with spiral main path cylindrical deflector analyzer.

5. Application

The spiral main path condenser offers to the designer a supplementary parameter μ, compared to the circular cylindrical plate condenser.

The resolution of the simplest configuration of time-of-flight mass spectrometer which includes a spiral main path condenser for energy spread dominated ion packets has been determined. By using the field-free space time-of-flight matrix elements of [4] the mass resolution $\Re$, takes the form:

$$\Re = \frac{\lambda_\gamma}{2(\lambda_s + \lambda_\delta \delta + \lambda_{\delta\delta}\delta^2)} \tag{20}$$

The meanings of the involved symbols are as follows: $\lambda_\gamma = v_0 T_\Sigma$, T_Σ the total flight time of the reference ion, λ_s the ion packet length at the source exit, λ_δ, $\lambda_{\delta\delta}$ the energy relative spread aberration coefficient of first and second order respectively. Other aberrations, including turn around time, were neglected. The ion packet width w at the detector is

$$w = A_y w_s + 2A_\alpha \alpha_s \tag{21}$$

where the index "s" means quantity at the source grid.

We consider the spiral cylinder time-of-flight mass spectrometer geometry having $\varphi = 120^\circ$, $\mu = -1.11542$, $l_1 = 0.92R$, $l_2 = 10^{-3}R$, $\lambda_\gamma = 1.7308R$, $\lambda_\delta = 0$, $\lambda_{\delta\delta} = 0.1492R$. It is equivalent as resolution with a homogeneous electric field single stage reflectron if $L = 0.8654R$. For the reflectron $\lambda_{\delta\delta} = 0.25L$, where L is the total ion field free path in the reflectron. The spiral cylinder compresses radially the ion packets to about a third the width at the source $A_y = -0.3397$ while for the reflectron $A_y = 1$.

A spiral main path TOF with $\varphi = 120^\circ$ but with $\mu = -1.43986$, $l_1 = 0.8$R and $l_2 = 1.87 \times 10^{-3}R$ focuses at second order in energy spread i.e., has $\lambda_\delta = \lambda_{\delta\delta} = 0$ and compresses to about 1/4 the initial width ($A_y = -0.2612$). It is to be compared to a two stage reflectron, also second order energy focusing, with say a velocity ratio $1/6^{1/2}$ (remaining part from v_0 at the reflectron intermediate grid after deceleration (see [8] for instance)). We expect to obtain the same resolution for the spiral cylinder and the reflectron if $R = 1.13172L$. The distance r at the exit of the condenser is rather small $5.586 \times 10^{-2}L$.

To velocity focus ions emitted from equipotential surfaces, a large variety of spiral cylinder geometries can be selected for delayed extraction operation. However, the $\lambda_\delta = 0$ configurations are excluded because the time lag becomes then infinite.

This kind of time-of-flight mass spectrometer has the following advantages: The absence of the two grids to be twice traversed by ions, compared with the two stage mirror, with at least 35% losses. Compact geometry compressing laterally the ion packets delivered from a wide ionization region, an alternative solution to the use of a cylindrical mirror [9].

6. Conclusions

The second order transfer matrix of the logarithmic spiral electrode condenser has been completed with the row of time-of-flight elements for the main field part as well as with the entry and exit ion path portions. Some advantages of the additional parameter μ can be capitalized as saving ion loss on grids and the lateral compression of the ion packets coming from large ion generating surfaces. These spiral cylinder TOF spectrometer can be an alternative of the cylindrical reflectron structures, a solution to concentrate negative ions generated in gas phase to small spots

Appendix A. Supplementary data

Supplementary data associated with this article can be found, in the online version, at doi:10.1016/j.ijms.2009.12.004.

References

[1] D. Ioanoviciu, Ion optics of electric deflectors with a spiral main path, Int. J. Mass Spectrom. 41 (1982) 229–239.
[2] D. Ioanoviciu, Ion optics, Adv. Electron. Electron Phys. 73 (1989) 1–92.
[3] M. Rachev, R. Srama, A. Srowig, E. Grün, Large area mass analyzer, Nucl. Instrum. Method A 535 (2004) 162–164.
[4] H. Matsuda, T. Matsuo, D. Ioanoviciu, H. Wollnik, V. Rabbel, Particle flight times through electrostatic and magnetic sector fields and quadrupoles to second order, Int. J. Mass Spectrom. Ion Phys. 42 (1982) 157–168.
[5] T. Sakurai, T. Matsuo, H. Matsuda, Particle flight times in a toroidal condenser and an electric quadrupole lens in the third order approximation, Int. J. Mass Spectrom. Ion Process. 68 (1986) 127–154.
[6] T. Matsuo, H. Matsuda, H. Wollnik, Particle trajectories in a toroidal condenser calculated in a third order approximation, Nucl. Instrum. Methods 103 (1972) 515–532.
[7] H. Wollnik, T. Matsuo, H. Matsuda, The electrostatic potential in a toroidal condenser, Nucl. Instrum. Methods 102 (1972) 13–17.
[8] D. Ioanoviciu, The application of ion optics in time-of-flight mass spectrometry, Int. J. Mass Spectrom. Ion Process. 131 (1994) 43–65.
[9] D. Ioanoviciu, C. Cuna, V. Cosma, I. Albert, E. Szilagyi, Design of a high-sensitivity negative ion source time-of-flight mass analyzer assembly created by cylindrical electrodes with a common axis, J. Mass Spectrom. 39 (2004) 1403–1407.